Applied Catalysis A: General 480 (2014) 42–49

Contents lists available at ScienceDirect

Applied Catalysis A: General

journal homepage: www.elsevier.com/locate/apcata

Influence of Na content on the catalytic properties of Pt-Ir/Al_2O_3 catalysts for selective ring opening of decalin

María A. Vicerich [a], Marcelo Oportus [b], Viviana M. Benitez [a], Patricio Reyes [b], Carlos L. Pieck [a,*]

[a] Instituto de Investigaciones en Catálisis y Petroquímica (INCAPE) (FIQ-UNL, CONICET), Santiago del Estero 2654, S3000AOJ, Santa Fe, Argentina
[b] Departamento de Físico Química, Facultad de Ciencias Químicas, Universidad de Concepción, Casilla 160-C, Concepción, Chile

ARTICLE INFO

Article history:
Received 23 December 2013
Received in revised form 16 April 2014
Accepted 21 April 2014
Available online 30 April 2014

Keywords:
Selective ring opening
Pt-Ir/Al_2O_3 catalysts
Na influence

ABSTRACT

The influence of the Na addition on Pt-Ir/Al_2O_3 on the reaction of selective ring opening of decalin and methyl cyclopentane was studied. The catalysts were evaluated by means of TPR, pyridine TPD, TEM, FTIR-CO and by the reaction tests of cyclohexane dehydrogenation, hydrogenolysis of cyclopentane, selective ring opening of decalin and methyl cyclopentane. It was found that Na strongly decreases the acidity and influences the metal properties of Pt-Ir/Al_2O_3 catalysts. The interaction between Pt and Ir is increased by the presence of Na, with larger metal crystals being obtained on the support modified by Na. As a consequence, the catalytic properties are also modified and the CP/CH ratio (parameter of demanding/not demanding reaction) is increased with sodium concentration. In the case of MCP reaction, Na strongly decreases the aromatic and *n*-C_6 formation and favors the selective reaction mechanism, thus favoring the formation of 2MP and 3MP. For the decalin reaction, it was found that the yield to the dehydrogenated product of the catalysts supported on Al_2O_3-Na is lower than that of the free Na-alumina supported catalyst, whereas the opposite occurs with the yield to C_1 due to the higher hydrogenolytic and lower dehydrogenation activity of the catalysts with Na. The yield to ring contraction (RC) products is higher on the catalyst without Na due to the higher acidity which favors the ring contraction reaction and the lower metallic activity; thus, the transformation of the RC product to ring opening products is decreased.

1. Introduction

The diesel production process is very complex and involves the selection and mixing of different oil fractions to meet certain specifications [1]. Diesel quality is measured by cetane number (CN). Quality combustion occurs when there is rapid ignition followed by a complete and uniform burning of fuel. The higher the CN, the lower the ignition delay and the better the quality of combustion. The incorporation of 0.5% additives (normally organic nitrates) increases the CN by 10 units, improves cold-start performance, reduces combustion noise and may reduce particulate matter (PM) emissions. Unfortunately, the additives increase the amounts of NOx emissions [2]. Diesel quality is affected by the presence of pollutants such as sulfur, which contributes to the emission of SOx. The aromatics content also affects the quality of diesel since it influences the combustion and particulate formation and emissions of polyaromatic hydrocarbons. By reducing the tenor of these compounds, a cleaner burning and increased cetane number may be obtained [2,3]. The reduction of sulfur and aromatics can be achieved with the use of technologies known as hydrotreating and hydrocracking [3]. One alternative is to transform the light cycle oil (LCO) stream in high quality diesel [4] because it represents approximately 10–20% of the product of FFC (catalytic cracking) and is sold as a product of little value for heating. The boiling range of the LCO is similar to that of gas-oil. However, it has a large amount of polycyclic aromatic compounds which makes its cetane number unacceptably low (<30). Therefore, the opening of at least one of the naphthene rings is needed to obtain a suitable cetane number.

Some noble metals such as Pt, Pd, Ir, Ru and Rh selectively activate the ring opening of cyclic hydrocarbons to produce corresponding paraffins with the same number of carbon atoms [5,6]. The experiments carried out in this work indicate that supported iridium catalysts are the most active ones since they have a low contribution of exocyclic C—C breaks, although the most suitable distribution of the rings occurs on rings of 5 carbon atoms. One solution is to promote ring contraction by means of a support

* Corresponding author. Tel.: +54 342 4533858; fax: +54 342 4531068.
E-mail address: pieck@fiq.unl.edu.ar (C.L. Pieck).

http://dx.doi.org/10.1016/j.apcata.2014.04.036
0926-860X/

having medium acidity. Industrial patents of SRO make use of iridium catalysts supported on medium acidity mesoporous supports controlled by the addition of alkali [7].

Electropositive promoters such as alkali and alkaline metals are often used as additives in heterogeneous catalysis to increase the catalytic activity, selectivity and/or stability. The ability of alkaline additives to modify the catalytic activity and/or selectivity can be understood by considering the effects induced on chemisorption properties of the metal surface. These effects may be originated from electronic interactions such as changing electron density due to the formation of alkali-metal species, and/or electrostatic interactions associated with alkali metal ions, and/or site blocking [8–10]. It is widely recognized that the electron density of a supported noble metal is increased by the addition of alkali and alkaline earth metals [11–15].

Other researchers also proposed different supports in order to improve the performance of the catalysts for SRO. Djeddi et al. [16], studying the SRO of MCP using Pt-Ir catalysts supported on TiO_2 in a wide reaction temperature range, found that all the catalysts have low selectivity to cracking products. On the other hand, Fe, Mo and Fe-Mo supported on silica mesoporous supports showed that the highly dispersed isolated tetrahedral entities and highly dispersed small FeO*x* nanoclusters have superior catalytic performance in the ring opening of MCP. Moreover, the synergy between Fe and Mo was not observed at low reaction temperatures (<200 °C) [17]. Tetralin hydroconversion over supported iridium catalysts on silica, alumina and amorphous silica-alumina supports has been investigated [18]. It was reported that the intermediate concentration of silica (40 wt%) leads to the highest activity and selectivity, in correlation with the Brønsted acidity measured by infrared spectroscopy of adsorbed pyridine. Indan ring opening was achieved with Ru-Pd/Al_2O_3 catalysts where the catalyst with Ru/Pd = 4 atomic ratio displayed the same high single cleavage selectivity and as low light formation as iridium [19]. McVicker et al. [20] reported the high activity and selectivity of the Ir/Al_2O_3 catalyst for RO of alkyl-substituted cyclopentanes and bicyclic naphthenes of C_5.

Resasco et al. [21] reported that in the case of the conversion of decalin on acidic catalysts, the acid function alone is not able to yield products with CN significantly higher than that of the decalin feed. For example, from decalin (CN = 36) by acid mechanism the product with higher CN is 2,3,6 trimethyl heptanes (CN = 30). Similarly, no significant gain in CN can be expected with hydrogenolysis metal catalysts operating via the dicarbene mechanism because the product with higher CN = 39 that could be obtained is 1,2 dipropyl cyclohexane. Only in the case of selective metal-catalyzed hydrogenolysis, with preferential cleavage at substituted C—C bonds, the predicted products have CN substantially higher than the decalin feed. For this reason, we study the influence of sodium content on Pt-Ir/Al_2O_3 on the conversion and selectivity of decalin. In other words, we try to perform the SRO of decalin using catalysts with low acidity in order to promote only the metal mechanism.

2. Experimental

2.1. Catalyst preparation methods

γ-Al_2O_3 (Cyanamid Ketjen CK-300; pore volume = 0.5 $cm^3\ g^{-1}$, Sg = 180 $m^2\ g^{-1}$, 35–80 mesh) was calcined for 4 h at 500 °C under flowing dry air. Firstly, a solution of NaOH on the support was added in order to obtain a desired concentration of Na (0.5, 1.0 and 1.5 wt%) and it was left at rest for 1 h. Then, support samples were left in contact with the amount of aqueous solutions of metallic precursors (H_2PtCl_6 and H_2IrCl_6) required for the desired metal loading for 2 h at room temperature in order to get a uniform distribution of metallic salts on the support particles. The resulting mixture was slowly dried at 70 °C until a dry solid was obtained. The drying process was completed in an oven (overnight at 120 °C) and the samples were then stabilized by calcination under flowing air for 4 h at 300 °C, and cooled down to ambient temperature under N_2. Samples were finally reduced under flowing H_2 at 500 °C for 4 h. All heating and cooling steps were set at 10 °C min^{-1}. The concentration of aqueous solutions of metallic precursor salts was adjusted to obtain the following metal loadings on the finished catalysts: 1.0%Pt-2%Ir-0.5%Na, 1.0%Pt-2%Ir-1.0%Na and 1.0%Pt-2%Ir-1.5%Na.

2.2. Analysis of metal contents

The Pt, Ir and Na contents of the catalysts were determined by inductively coupled plasma-optical emission spectroscopy equipment (ICP-OES) (Perkin Elmer, Optima 2100 DV) after acid digestion.

2.3. Temperature-programmed reduction (TPR)

This technique allows gathering information about the interaction of the metal components by means of the measurement of the hydrogen consumption during the reduction of the oxides at constant heating rate. The temperature at which reduction occurs and the number of reduction peaks depend on the oxidation state of the metals, the interaction of the oxides among them and with the support, and the possible catalytic action of Pt or other elements present or generated during reduction. These tests were performed in an Ohkura TP2002 equipment provided with a thermal conductivity detector. At the beginning of each TPR test, the catalyst samples were pretreated in situ by heating under flowing air at 350 °C for 1 h. Then, they were heated from room temperature to 700 °C at 10 °C min^{-1} in a controlled gas stream of 5.0% hydrogen in argon.

2.4. Temperature-programmed desorption of pyridine (TPD)

The amount and strength distribution of acid sites were assessed by means of the temperature-programmed desorption of pyridine (Py). 200 mg of catalyst was first immersed in a closed vial containing pure pyridine (Merck (99.9%)) for 4 h. Then the vial was opened and the excess base was allowed to evaporate at room conditions until apparent dryness. The sample was then loaded into a quartz tube of 0.4 cm diameter over a quartz wool plug. A constant flow of nitrogen (40 $cm^3\ min^{-1}$) was kept through the sample. A first step of desorption of weakly physisorbed base and sample stabilization was performed by heating the sample at 110 °C for 2 h. Then, the temperature of the oven was raised to a final value of 550 °C at a heating rate of 10 °C min^{-1}. The reactor outlet was directly connected to a flame ionization detector. The detector signal (in mV units) was sampled at 1 Hz and recorded in a computer device.

2.5. Transmission electron microscopy

Transmission electron micrographs (TEM) and electron diffraction patterns (ED) were obtained in a Jeol JEM 1200 EXII microscope. The supported catalysts were ground in an Agatha mortar and dispersed in ethanol. A diluted drop of each dispersion was placed on a 150 mesh copper grid coated with carbon.

2.6. Fourier transformed infrared (FTIR) spectroscopy of chemisorbed CO

FTIR spectra of adsorbed CO were obtained in order to study the effect of Ir deposition on the properties of the metal function. The spectra of chemisorbed CO for the prepared catalysts

were recorded within the wavenumber range of 4000–1000 cm^{-1}. A Shimadzu Prestige-21 spectrometer with a spectral resolution of 4 cm^{-1} was used. Spectra were recorded at room temperature and self-supported wafers with a diameter of 16 mm and a weight of 20–25 mg were used. The experimental procedure was as follows: catalyst samples were reduced in a hydrogen flow at 400 °C (reached at a 10 °C min^{-1} heating rate) for 30 min. Samples were then outgassed at 2.7×10^{-3} Pa and 400 °C for 120 min. After an initial (I) spectrum had been recorded, the samples were exposed to a CO pressure of 4000 Pa for 5 min and then a second (II) FTIR spectrum was recorded. The chemisorbed CO absorbance for each sample was obtained by subtracting spectrum I from spectrum II.

2.7. Cyclopentane hydrogenolysis (CP)

The reaction was performed in a glass reactor (length 10 cm, diameter 1 cm) under the following conditions: catalyst mass 150 mg, temperature 270 °C, pressure 0.1 MPa, H_2 flow rate 40 cm^3 min^{-1}, cyclopentane flow rate 0.483 cm^3 h^{-1}. Cyclopentane was fed to the reactor using a Sage Instruments 341B syringe pump. Before the reaction was started, the catalysts were treated in H_2 (60 cm^3 min^{-1}, 270 °C, 1 h). The reaction products were analyzed by online gas chromatography using a ZB-1 capillary column. The error in the conversion value in the CP hydrogenolysis test is about 8%. Only values of initial conversion at 5 min time-on-stream are reported.

2.8. Cyclohexane dehydrogenation (CH)

The reaction was performed in a glass reactor (length 10 cm, diameter 1 cm) under the following conditions: catalyst mass 50 mg, temperature 300 °C, pressure 0.1 MPa, H_2 flow rate 80 cm^3 min^{-1} and cyclohexane flow rate 1.61 cm^3 h^{-1}. Sage Instruments 341B syringe pump was used to introduce the cyclohexane into the reactor. Before the reaction was started, the catalysts were treated in H_2 (80 cm^3 min^{-1}, 500 °C 1 h). The reaction products were analyzed by online gas chromatography using a ZB-1 capillary column. All points reported are mean values obtained by averaging 12 consecutive measurements equally spaced along the run. No significant catalyst deactivation was observed in any run. The average error was less than 3%.

2.9. Methylcyclopentane ring opening (MCP)

Before the reaction, samples were reduced at 250 °C for 1 h. The conditions used were: mass = 135 mg, H_2 flow rate = 36 cm^3 min^{-1}, MCP flow = 0.362 cm^3 min^{-1}, reaction temperature = 250 °C and time = 2 h. The reaction products were analyzed on a Varian CX 3400 gas chromatograph equipped with a capillary column Phenomenex ZB-1 connected online.

2.10. SRO of decalin

All SRO experiments were performed in a stainless steel, autoclave-type stirred reactor. The reaction conditions were: temperature = 300–325–350 °C, hydrogen pressure = 3 MPa, stirring rate = 1360 rpm, volume of decalin = 25 cm^3, catalyst loading = 1 g and reaction time = 6 h. A sample was taken at the end of the experiments and it was analyzed using a Varian 3400 CX gas chromatograph equipped with a capillary column (Phenomenex ZB-5) and FID.

3. Results and discussion

Fig. 1 shows the TPR profiles of monometallic Pt and Ir catalysts with and without 1 wt% of Na. The monometallic Pt catalyst has a pronounced reduction peak at ca. 200 °C and a minor reduction band between 250 and 300 °C. This reduction pattern has been frequently observed by several authors [22–24] and it is generally accepted that the first peak is due to the reduction of Pt oxide species weakly interacting with alumina. The less important second reduction band is assigned to the reduction of Pt oxychlorinated species in strong interaction with the support [25]. It can be seen that the monometallic Ir catalyst has a big peak centered about 240 °C as reported elsewhere [26]. This peak begins at 150 °C, finishes at 350 °C and has a shoulder at 260 °C. The broad reduction zone evidences the different interactions between the Ir oxides species and the support and the different particle sizes of the Ir oxide agglomerates. The Na addition shifts the reduction peaks, and the Pt-Na catalyst has a broad reduction peak which is centered at 240 °C. This could be due to the fact that Na inhibits the hydrogen spillover interfering in the reduction of the metals [26]. However, an opposite effect can be seen over the monometallic Ir catalyst. Probably, Na produces a strong decrease of support acidity leading to weak metal–support interaction.

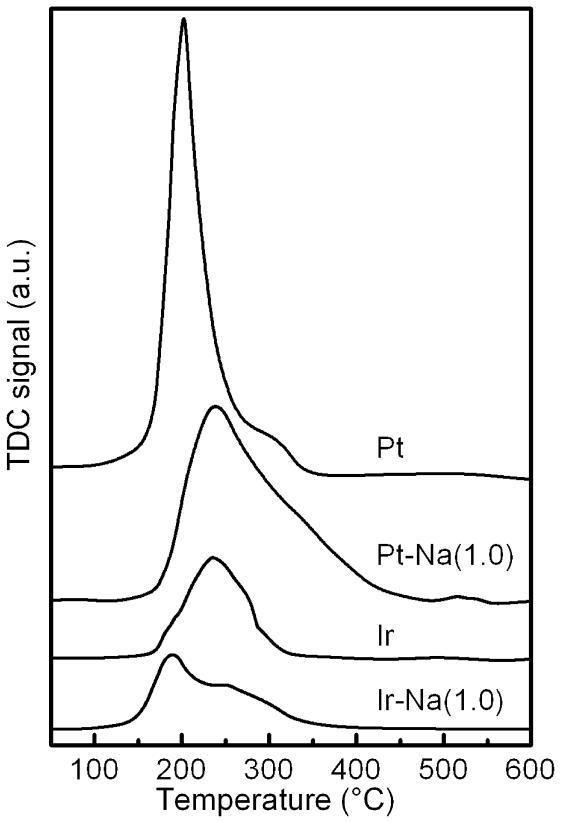

Fig. 1. TPR profiles of Pt and Ir monometallic catalysts with and without Na.

Fig. 2 shows the TPR profiles of Pt(1.0)-Ir(2.0)/Al_2O_3-Na(x) catalysts. The bimetallic Pt-Ir/Al_2O_3 catalyst has a reduction peak close to 200 °C due to a simultaneous reduction of Pt and Ir oxides making clear the strong Pt-Ir interaction. Sodium addition shifts slightly the reduction peak to a lower temperature which can be attributed to a decrease of support acidity. As a consequence, the metal–support interaction is decreased making it easier to reduce metal oxides. On the other hand, as mentioned above, Na inhibits the hydrogen spillover interfering in the reduction of the metals [26]. These two opposite phenomena which lead to the addition of sodium cause a slight displacement of the reduction peaks. In spite of the catalyst with 1.5% sodium no peak shift was observed with respect to the catalyst without sodium. It is important to note that in this latter catalyst, the formation of a shoulder in the reduction peak

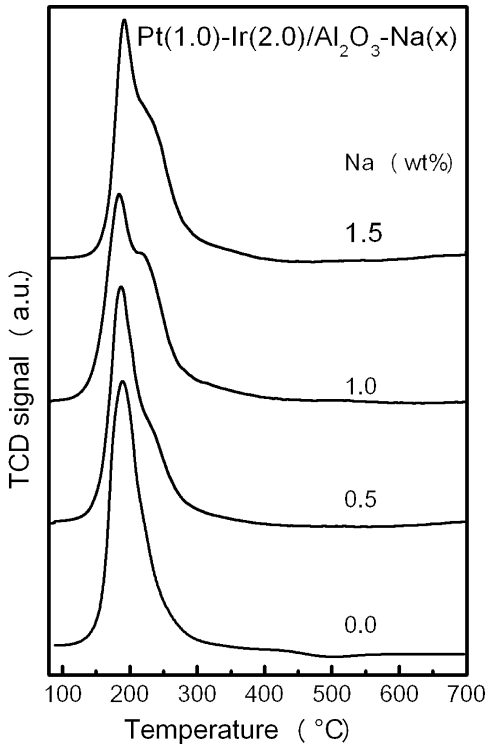

Fig. 2. TPR profiles of bimetallic catalysts with different Na contents.

is observed, which intensifies by increasing the amount of Na. This can be attributed to the reduction of Pt species in strong interaction with Na, as shown in Fig. 1.

The pyridine thermodesorption technique provides valuable information about the acidity and acid strength distribution of solid catalysts. The area under the desorption curves is proportional to total acidity. Table 1 shows the areas relative to the sodium-free catalyst. As expected, the acidity decreases with increasing Na content because they neutralize the acid sites of alumina. Furthermore, the TPD profiles (no shown) revealed that the strength of the sites is not significantly modified by Na addition because the temperature desorption of pyridine is similar for all the catalysts. This indicates that Na neutralizes the strengths and weaknesses of acid sites.

Fig. 3 shows the particle size distribution of the Pt (1.0)-Ir (2.0)/Al_2O_3-Na(x) catalysts. It can be observed that with increasing sodium concentration there is an increase in the metal particle size. This can be explained considering that as sodium hydroxide neutralizes the acid sites of the alumina support, it decreases the metal–support interaction and, therefore, during the reduction step, an enhancement in the metal particle size can occur. It can be noted that the distribution of the particles of the catalyst with 1.5 wt% of Na has a significant fraction of particles in the 2–2.5 nm range. This agrees with the TPR where the appearance of a shoulder can be observed at a higher temperature reduction of the catalysts with higher sodium content.

Table 1
Normalized pyridine TPD areas, average cyclohexane conversion and cyclopentane conversion at 5 min time-on-stream for Pt(1)-Ir(2.0)/Al_2O_3-Na(x) catalysts.

Catalyst Na (wt%)	Pyridine TPD areas	CP conversion (%)	CH conversion (%)	CP/CH
0.0	1.00	94.0	44.7	2.10
0.5	0.74	97.9	37.4	2.62
1.0	0.36	88.9	32.0	2.78
1.5	0.23	96.2	25.4	3.79

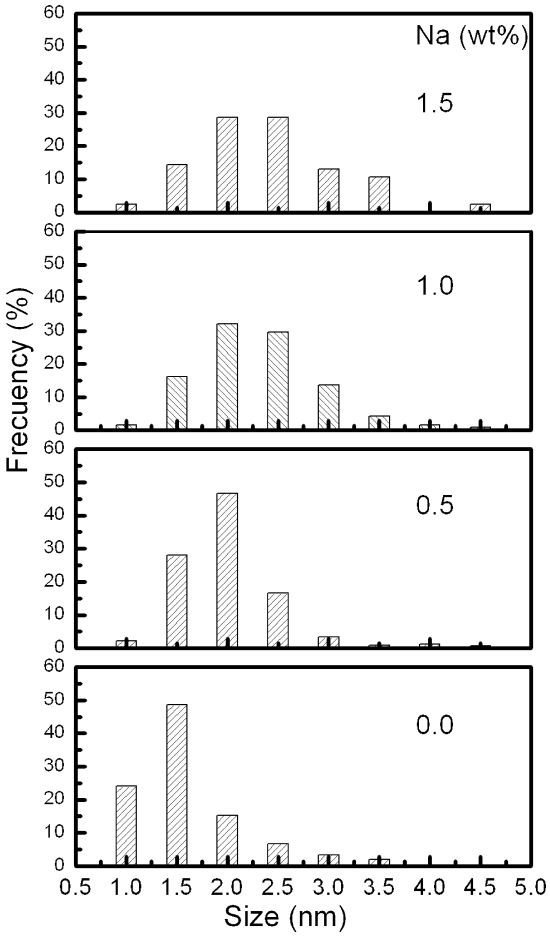

Fig. 3. Particle size distribution obtained by TEM of the bimetallic catalysts with different Na contents.

The interaction between the metals was also studied by FTIR-CO spectroscopy. Fig. 4 shows the IR spectra at 30 Torr in the 1850–2150 cm^{-1} wavelength range for the monometallic and bimetallic catalysts under study. Fig. 4 shows only the wave number region corresponding to linear CO because the band due to CO adsorbed in the bridge form, Pt_2CO, was too small to be studied. It can be seen that the monometallic Pt/Al_2O_3 catalyst shows an absorption peak at 2085 cm^{-1} which corresponds to the adsorption of linear CO on Pt [27–29]. The adsorption peak shifts to a lower frequency (2077 cm^{-1}) on the Pt-Na/Al_2O_3 catalyst. Similar results were reported by Shimizu et al. [30] on Pt-Na/SiO_2 catalysts. They attributed the shift to lower frequency to an increase in the electron density of Pt by Na. They also proposed that the electron charge of the Pt metal particles increases as the amount of electropositive modifier (Na) increases as a result of the increased electron charge of the oxygen atoms on the support. The increase in the electron density of the Pt metal particles may be partially attributed to the direct electron donation from Na to the Pt metal particles.

The monometallic Ir/Al_2O_3 catalyst shows two absorption bands centered about at 2087 and 2020 cm^{-1}. The incorporation of Na shifts the absorption peak to 2064 cm^{-1} while the other peak at 2020 cm^{-1} disappears. Adsorption of CO on Ir/Al_2O_3 was studied by Solymosi et al. [31]; they attributed a band at 2080–2050 cm^{-1} to the presence of Ir–CO complexes.

Three bands have been identified in the 2100–1900 cm^{-1} range on the FTIR-CO of Ir catalysts [32–38]. Those at 2087 and 2020 cm^{-1} correspond to linearly bonded CO adsorbed either on large and small Ir particles [33] or over high- (planes) and low-coordinated (edges, corners, etc.) Ir sites [39], respectively. The disappearance

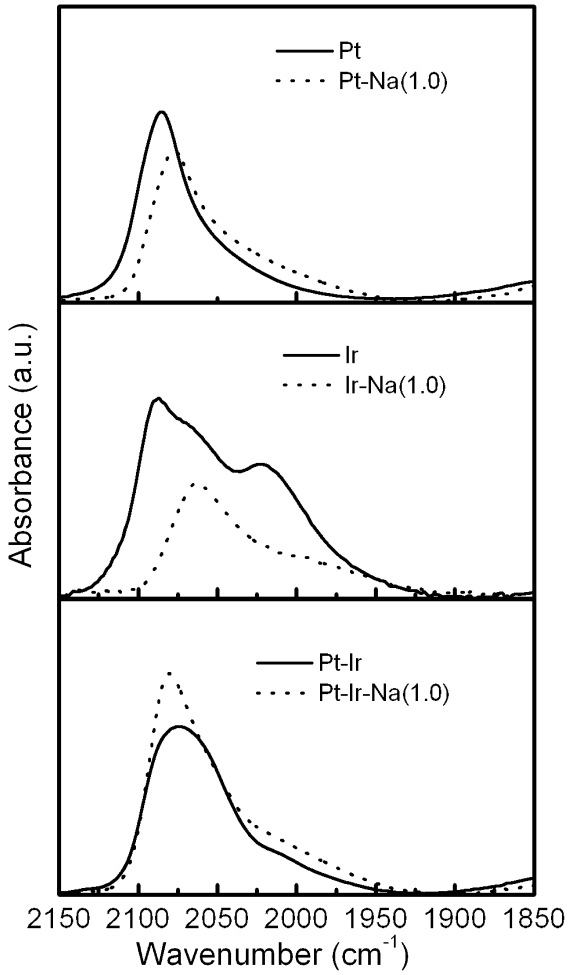

Fig. 4. FTIR spectra of CO adsorbed on monometallic and bimetallic catalysts with and without Na at 30 Torr.

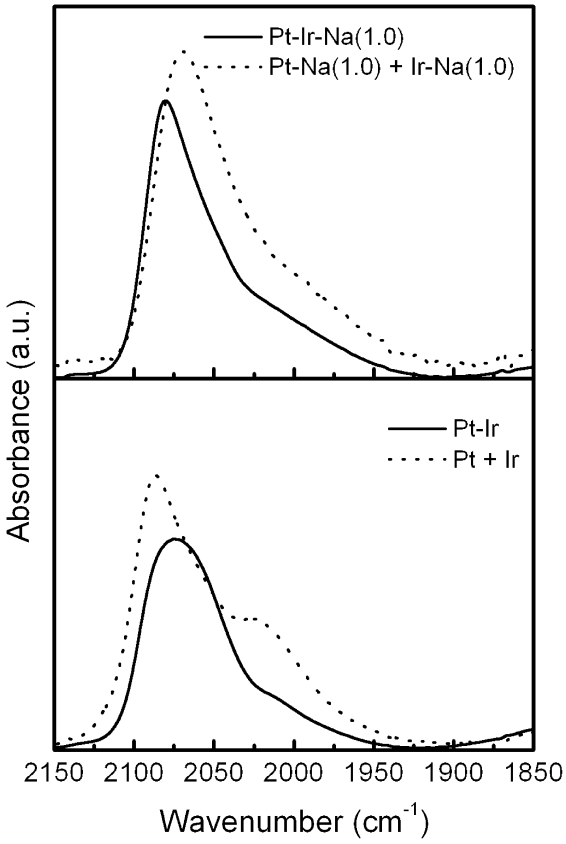

Fig. 5. FTIR spectra of CO adsorbed on bimetallic catalysts with and without Na at 30 Torr and the sum of the spectrum of monometallic Pt and Ir catalysts with and without Na.

of the absorption band at 2020 cm^{-1} due to Na addition can be explained by an increase of crystal size while the shift to lower frequencies by an increase of the electron density of the Ir metal particles in a similar way to Pt/Al_2O_3 catalysts.

The influence of Na on bimetallic catalysts is apparently less important because the shift to lower frequencies occurs only to a slight extent. The absorption peak of the bimetallic catalysts (with and without Na) appears at about 2075–2078 cm^{-1}. It is interesting to compare the absorption peaks of the bimetallic catalysts with the corresponding spectrum obtained by the sum of monometallic catalysts (Fig. 5). The absorption peak at 2020 cm^{-1} due to Ir is not observed on the bimetallic $Pt\text{-}Ir/Al_2O_3$ catalyst. Moreover, the absorption peak of Pt is shifted from 2087 to 2073 cm^{-1}. In the case of the promoted Na catalyst, there are shifts from 2069 cm^{-1} (spectrum due to the sum on monometallic Pt and Ir catalysts) to 2082 cm^{-1} (bimetallic $Pt\text{-}Ir/Al_2O_3$-Na(1.0%) catalyst). These results indicate a strong interaction between Pt and Ir. In a previous work, we confirmed the existence of a strong interaction between Pt and Ir on alumina supported catalysts by TEM [40]. These results are consistent with TPR experiments where a strong interaction between Pt and Ir was observed. Moreover, they are in agreement with the results of CO FTIR absorption.

Table 1 shows the conversion values of the reactions of hydrogenolysis of cyclopentane and cyclohexane dehydrogenation. Boudart et al. [41,42] classified catalytic reactions as "demanding" (sensitive to morphological structure) and "facile" (structure-insensitive), according to the requirement or not of a particular ensemble of neighboring metal atoms in order to form adsorbate bonds with the proper strength. The geometric model has been refined as "ensemble-size" model [43–45] on the assumption that reaction rates are proportional to the probability of finding particular groups of neighboring atoms. Two classical test reactions are used that have an entirely different behavior according to the geometric factor theory: cyclopentane (CP) hydrogenolysis, which is a demanding one [46], and cyclohexane (CH) dehydrogenation which is non-demanding under the used experimental conditions [41].

It can be seen that the conversion of cyclohexane decreases as the Na concentration of the support increases whereas the cyclopentane conversion does not change significantly. Consequently, the CP/CH (parameter of demanding/not demanding reaction) ratio increases with sodium concentration.

Both reactions are only catalyzed by the metal function; therefore, the variation can be attributed to the way in which the Na interacts with the active phase (Pt-Ir), and how Na would alter the interaction between the two metals. Sodium in interaction with the active phase may, by a simple geometric effect, prevent the adsorption of hydrocarbons. In this case, the hydrogenolysis reaction should be the most affected one because it is a demanding reaction. As a consequence, the CP/CH ratio should decrease with increasing Na concentration. The interaction of sodium with the active phase (Pt-Ir) should also produce a change in the electronic structure of metals by changing the catalytic activity for both reactions. Finally, Na could favor the formation of large ensembles of Pt and Ir as it was asserted by TEM analysis.

The lower dehydrogenation activity as sodium increases is explained by an increased particle size of Pt and Ir since the dehydrogenation of cyclohexane is not a demanding reaction whereas

the hydrogenolysis reaction of CP would be benefited. Large crystals of Pt and Ir are more active than small particles since hydrogenolysis is a demanding reaction. The conversion of cyclopentane on the hydrogenolysis reaction does not change. The increased size of the metal particles causes an increase in the conversion by atom exposed but the amount of superficial atoms is reduced.

The results obtained agree with those of TPR and TEM which show that sodium favors the formation of large ensembles of Pt-Ir. However, the electronic effect of sodium should not be discarded because the increased size of the particles is not enough to explain the observed behavior. Some authors reported a partial covering of Pt surface by NaO*x* on Pt/TiO_2 catalysts [47] and Pt/SiO_2 catalysts [30]. For K-loaded Pt/Al_2O_3, Busca et al. also proposed that Pt centers lie in close proximity of potassium oxide species [48]. Shimizu et al. [30] found that the electron charge of the Pt atoms increases as the amount of the electropositive modifier (Na) increases.

The ring opening reaction of methylcyclopentane produces branched paraffins (2-methylpentane, 3-methylpentane) and linear paraffins (*n*-hexane). Differences in the distribution of the ring opening products of MCP are attributed to the intrinsic nature of the metals, metal dispersion, the nature of the support, the hydrocarbon adsorption mode on metals and experimental conditions [46]. In Pt/Al_2O_3 highly dispersed catalysts ($d < 2$ nm) breaking substituted C—C bonds are favored since the π allyl mechanism, which requires a flat adsorption of three neighboring carbon atoms, interacts with a single-metal site. Therefore, the products obtained from the opening of the MCP in highly dispersed catalysts are 2-methylpentane, 3-methylpentane and *n*-hexane. In the Pt/Al_2O_3 catalyst with lower dispersion ($d > 2$ nm), the preferential rupture of unsubstituted C—C bond takes place. This can be attributed to a dicarbene mechanism where two endocyclic carbon atoms are involved with adjacent metal atoms. In this case, the reaction products are only 2-methylpentane and 3-methylpentane while *n*-hexane is not formed. In the case of Ir catalysts the reaction was found insensitive to the dispersion (only 2-methylpentane and 3-methylpentane are obtained) [46,49]. Furthermore, Ir catalysts showed a tendency to break endocyclic C—C bonds of MCP [30]. In this case, the ring opening of MCP takes place primarily through a mechanism in which the intermediate dicarbenes are adsorbed perpendicular to the metal surface. van Senden et al. [49] using iridium catalysts with different dispersion reported that the opening of endocyclic C—C bond of MCP occurs when the catalysts were covered with carbonaceous species [50]. Contrary to Ir supported on alumina where the break occurs on substituted endocyclic C—C bonds, on Ir supported on SiO_2 it was observed that the predominant mechanism was dicarbene [51]. The literature remarks that the reactivity of iridium is much higher than that of Pt [52] although the catalytic results did not confirm major differences in the reaction rate [53]. Maire et al. [54] concluded that the product distribution in RO reactions depends on the operating reaction mechanisms. According to a non-selective reaction path that would occur on small metallic particles, with the same breaking probability as any of the cyclic bonds, a product ratio *n*-C_6:2MP:3MP of 2:2:1 is expected. On the other hand, if a selective mechanism where the breaking of substituted endocyclic bonds is forbidden operates, such products ratio would be 0:2:1. Such mechanism would proceed on metallic aggregates of higher size. An alternative mechanism, partially selective, with an intermediate product distribution ratio, can also be possible.

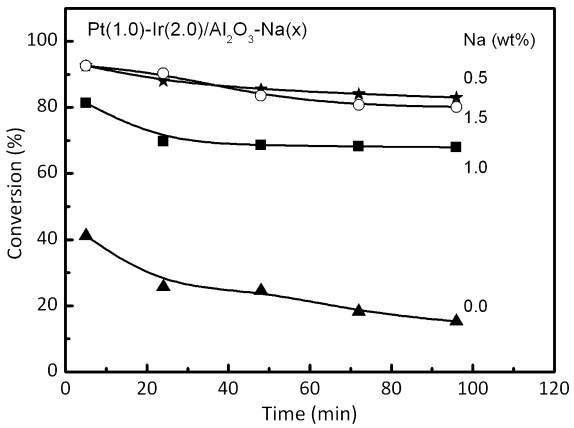

Fig. 6. Conversion values as a function of time obtained in the MCP reaction of Pt(1.0)-Ir(2.0)/Al_2O_3-Na(*x*) catalysts.

Fig. 6 shows the conversion values as a function of time obtained in the MCP reaction of Pt(1.0)-Ir(2.0)/Al_2O_3-Na(*x*) catalysts. It can be seen that the conversion decreases with reaction time due to the deposition of coke in all the catalysts. Moreover, it is observed that the catalysts supported on Al_2O_3 with sodium have a higher activity than the catalyst without sodium. However, the increased activity is not directly related to the sodium content or to the cyclohexane dehydrogenation as well as with acidity but it has a direct relation with the cyclopentane hydrogenolysis activity reported in Table 1 for the catalyst without Na. That means the reaction is controlled by the metal function mainly by the hydrogenolytic character of the metal phase.

The values of selectivities towards reaction products taken at 15 min of time on stream (i.e. with very low amount of coke deposited on catalyst surface) are shown in Table 2. It can be observed that the Pt-Ir catalyst without Na have a high selectivity towards benzene and *n*-C_6 while the Na promoted catalysts produce a low amount of these compounds. The formation of aromatics on noble metal supported catalysts was studied by Ponec et al. [55]. They were able to determine the contribution of metal and acid sites of sulfur modified Pt/Al_2O_3, $Pt\text{-}Co/Al_2O_3$ and $Pt\text{-}Re/Al_2O_3$ catalysts and found that cyclohexane, benzene and *n*-C_6 required the presence of both metal and acid sites. Then, in the catalyst with Na the reaction can be assumed to proceed through a bifunctional mechanism producing benzene and *n*-C_6. On the other hand, the low acidity of the catalysts with Na (Table 1) leads to a low formation of *n*-C_6 and benzene.

It is interesting to analyze the selectivity to C_1 and C_2–C_5. C_1 is formed mainly by hydrogenolysis reaction on the metal function while C_2–C_5 products are generated by cracking on the acid function. The results clearly show that the addition of Na decreases the cracking activity while the metal function is improved. These results are in agreement with the lower acidity

Table 2
Selectivity to 2MP, 3MP, *n*-C_6, C_1–C_5 and benzene (Bz) in the reaction of SRO of MCP at 15 min time on stream of Pt(1)-Ir(2.0)/Al_2O_3-Na(*x*).

Catalyst	Selectivity (%)							Molar ratio	
Na (wt%)	2MP	3MP	*n*-C_6	C_1	C_2–C_5	Bz	RO	*n*-C_6/3MP	2MP/3MP
0.0	25.6	16.4	12.8	0.4	18.0	26.8	81.6	0.78	1.56
0.5	60.1	26.2	3.3	2.6	7.1	0.7	90.3	0.13	2.29
1.0	58.9	22.8	2.3	4.6	10.3	1.1	85.1	0.10	2.58
1.5	58.2	23.0	2.6	3.0	12.4	0.8	85.6	0.16	2.53

Table 3
Decalin conversion, percentage of cis and trans decalin and selectivity to different reaction products after 6 h of reaction for Pt(1)-Ir(2.0)/Al_2O_3-Na(x) catalysts.

Catalyst Na (wt%)	T (°C)	X (%)	Trans (%)	Cis (%)	Yield (%)			
					CR	RO	RC	DH
0.0	300	7.1	82.5	10.4	2.9	23.2	60.9	13.0
	325	10.1	77.9	12.0	5.0	40.6	35.6	18.8
	350	28.5	61.2	10.3	9.8	28.6	23.8	38.8
0.5	300	11.6	78.2	10.2	11.3	31.8	44.3	12.6
	325	30.4	60.7	8.9	19.5	45.0	20.0	15.5
	350	40.4	48.1	11.5	22.2	38.6	20.5	18.7
1.0	300	10.8	78.7	10.5	11.0	36.2	42.5	10.3
	325	17.7	72.6	9.7	10.8	30.4	44.2	14.6
	350	37.1	54.2	8.7	14.9	32.3	32.0	20.8
1.5	300	13.4	78.1	8.5	14.5	28.2	46.0	11.3
	325	16.6	72.3	11.1	11.2	32.4	44.0	12.4
	350	43.9	48.7	7.4	20.0	38.8	14.5	26.7

T: reaction temperature; X: conversion.

and higher hydrogenolytic activity of the Na promoted catalysts with respect to the catalyst without Na, as reported in Table 1.

It can be seen that all the catalysts supported on Al_2O_3-Na produce lower amounts of n-C_6 than the catalyst without sodium. n-C_6 should not be produced on large particles of metal according to the selective model. Moreover, the 2MP/3MP ratio is close to 2 according to the selective model. These results are in agreement with the increased size of the metal particles of the catalysts supported on Al_2O_3-Na, as shown in Fig. 3. Finally, it can be seen in Table 2 that catalysts supported on Al_2O_3-Na exhibit higher selectivity to ring opening products (RO) than the Na-free counterpart. This can be explained by taking into account the lower acidity of Pt and Ir supported on Al_2O_3-Na. The suppressed cracking activity of these catalysts reduces the rate of destruction of ring opening products.

The results of decalin conversion and the percentage of cis and trans-decalin obtained after 6 h of reaction at different reaction temperatures are shown in Table 3. The decalin used in the experiments has a 37.5% cis, thus a trans/cis ratio = 1.63. It can be seen in Table 3 that the trans/cis ratio is higher than the initial ratio (1.63). Higher trans/cis ratios can be due to the higher reactivity of the cis isomer [56,57] and isomerization reactions of cis/trans [58]. It is known that cis-decalin in more selective to RO products than trans-decalin which is converted to cracking products [56]. The cis/trans thermodynamic equilibrium composition (10–90 vs. 40–60 in the starting decalin) is rapidly reached, resulting in an enrichment of the reactant mixture in trans-decalin. On the other hand, as expected, the conversion increased as the reaction temperature increased and the catalysts with Na are more active than the catalyst without Na as found in the MCP reaction (Fig. 6). These results demonstrate the importance of the metallic phase for decalin transformation because the conversion is increased when the acidity is decreased.

As decalin conversion leads to a complex mixture of more than 200 compounds, the decalin reaction products were classified according to the same criterion used in previous work [59]. The products of reaction are classified into cracking products (C_1–C_9 products); ring opening (RO) C_{10} products; ring contraction (RC); naphthalene and other products including heavy dehydrogenation products.

Table 3 shows the selectivity values obtained from the reaction of decalin SRO. The best results were obtained with catalyst Pt(1.0)-Ir(2.0)-0.5% Na at the temperature of 325 °C. The formation of cracking products increases with the reaction temperature in all the catalysts studied because it is a reaction with high activation energy [60]. As expected, the increase in reaction temperature also favors the formation of dehydrogenated products because the dehydrogenation is an endothermic and reversible reaction [60].

The yield to ring opening products (defined as the selectivity to RO products × conversion/100) depends upon the reaction temperature, the acidity of the support and the metal charge. An increase of the temperature, acidity and metal charge promotes the formation of ring opening compounds; however, it may also favor cracking and dehydrogenation reactions that decrease the product selectivity desired. The yield to dehydrogenated product of the catalysts supported on Al_2O_3-Na is lower than that obtained in free Na, in agreement with cyclohexane dehydrogenation conversion reported in Table 1. The yield to cracking products (CR) is higher on the catalysts promoted with Na. Taking into account that cracking reactions are catalyzed by the strong acid sites of the support; the yield to CR products shown in Table 3 is opposed to the expected one. This is indicating that CR products are also formed by the metallic function, which is more active on the Na promoted catalysts (Table 1).

The yield to RC products is higher in the catalyst without Na because a higher acidity favors the ring contraction reaction and a lower metallic activity suppresses the conversion of RC products into RO ones.

4. Conclusions

The results of the catalysts characterization show that Na strongly decreases the acidity and influences the metal properties of Pt-Ir/Al_2O_3 catalysts. The interaction between Pt and Ir is increased by the presence of Na. Larger metal crystals are obtained on the support modified by Na. As a consequence, the catalytic properties are also modified, the CP/CH ratio (parameter of demanding/not demanding reaction) being increased with sodium concentration. In the MCP reaction, Na strongly decreases the aromatics yield and n-C_6 formation and favors the selective reaction mechanism favoring the formation of 2MP and 3MP. In the decalin reaction it was found that the yield to dehydrogenated products of the catalysts supported on Al_2O_3-Na is lower than that of the free Na-alumina supported catalyst whereas the opposite occurs with the yield to C_1 due to the higher hydrogenolytic and lower dehydrogenation activity of the catalysts with Na. The yield to ring contraction (RC) products is higher in the catalyst without Na due to the higher acidity which favors the ring contraction reaction and the lower metallic activity; thus, the transformation of RC products into ring opening products is decreased.

Acknowledgment

Thanks are given to Elsa Grimaldi for the English language editing.

References

[1] Kirk-Othmer, Encyclopedia of Chemical Technology, vol. 17, 3rd ed., John Wiley & Sons, Inc., USA, 1982, pp. 119–143.
[2] J.H. Gary, G.E. Handwerk, Petroleum Refining: Technology and Economics, Marcel Dekker, Inc., New York, 1994.
[3] T.C. Kaufmann, A. Kaldor, G.F. Stuntz, M.C. Kerby, L.L. Ansell, Catal. Today 62 (2000) 77–90.
[4] V. Calemma, R. Giardino, M. Ferrari, Fuel Process. Technol. 91 (2010) 770–776.
[5] H. Du, C. Fairbridge, H. Yang, Z. Ring, Appl. Catal. A: Gen. 294 (2005) 1–21.
[6] P. Samoila, M. Boutzeloit, C. Especel, F. Epron, P. Marécot, J. Catal. 276 (2010) 237–248.
[7] K. Shimizu, T. Sunagawa, C.R. Vera, K. Ukegawa, Appl. Catal. A: Gen. 206 (2001) 79–86.
[8] J. Benzinger, R.J. Madix, Surf. Sci. 94 (1980) 119–153.
[9] D. Heskett, Surf. Sci. 199 (1988) 67–86.
[10] E.L. Garfunkel, J.E. Crowell, G.A. Somorjai, J. Phys. Chem. 86 (1982) 310–312.
[11] H. Yoshitake, Y. Iwasawa, J. Phys. Chem. 96 (1992) 1329–1334.
[12] H. Yoshitake, Y. Iwasawa, J. Catal. 131 (1991) 276–284.
[13] H. Yoshitake, Y. Iwasawa, J. Phys. Chem. 95 (1991) 7368–7372.
[14] T. Visser, T.A. Nijhuis, A.M.J. van der Eerden, K. Jenken, Y. Ji, W. Bras, S. Nikitenko, Y. Ikeda, M. Lepage, B.M. Weckhuysen, J. Phys. Chem. B 109 (2005) 3822–3831.
[15] M. Lepage, T. Visser, F. Soulimani, A.M. Beale, A. Iglesias-Juez, A.M.J. van der Eerden, B.M. Weckhuysen, J. Phys. Chem. C 112 (2008) 9394–9404.
[16] A. Djeddi, I. Fechete, F. Garin, Top. Catal. 55 (2012) 700–709.
[17] A. Boulaoued, I. Fechete, B. Donnio, M. Bernard, P. Turek, F. Garin, Microporous Mesoporous Mater. 155 (2012) 131–142.
[18] S. Nassreddine, S. Casu, J.L. Zotin, C. Geantet, L. Piccolo, Catal. Sci. Technol. 1 (2011) 408–412.
[19] J. Shen, N. Semagina, ACS Catal. 4 (2014) 268–279.
[20] G.B. McVicker, M. Daage, M.S. Touvelle, C.W. Hudson, D.P. Klein, W.C. Baird Jr., B.R. Cook, J.G. Chen, S. Hantzer, D.E.W. Vaughan, E.S. Ellis, O.C. Feeley, J. Catal. 210 (2002) 137–148.
[21] R.C. Santana, P.T. Do, M. Santikunaporn, W.E. Alvarez, J.D. Taylor, E.L. Sughrue, D.E. Resasco, Fuel 85 (2006) 643–656.
[22] S.M. Agustine, W.M.H. Sachtler, J. Catal. 116 (1989) 184–194.
[23] H. Lieske, G. Lietz, H. Spindler, J. Völter, J. Catal. 81 (1983) 8–16.
[24] G. Lietz, H. Lieske, H. Spindler, W. Hanke, J. Völter, J. Catal. 81 (1983) 17–25.
[25] L.S. Carvalho, C.L. Pieck, M.C. Rangel, N.S. Fígoli, J.M. Grau, P. Reyes, J.M. Parera, Appl. Catal. A: Gen. 269 (2004) 91–103.
[26] C. Carnevillier, F. Epron, P. Marecot, Appl. Catal. A: Gen. 275 (2004) 25–33.
[27] J.A. Anderson, C.H. Rochester, Catal. Today 10 (1991) 275–282.
[28] F. Boccuzzi, G. Ghiotti, A. Chiorino, L. Marchese, Surf. Sci. 233 (1990) 141–152.
[29] J.A. Anderson, M.G.V. Mordente, C.H. Rochester, Chem. Soc. Faraday Trans. 1 (85) (1989) 2983–2990.
[30] K. Shimizu, K. Shimura, K. Kato, N. Tamagawa, M. Tamura, A. Satsuma, J. Mol. Catal. A: Chem. 353–354 (2012) 171–177.
[31] F. Solymosi, E. Novak, A. Molnar, J. Phys. Chem. 94 (1990) 7250–7255.
[32] A.B. Dongil, B. Bachiller-Baeza, I. Rodríguez-Ramos, A. Guerrero-Ruiz, C. Mondelli, A. Baikerm, Appl. Catal. A: Gen. 451 (2013) 14–20.
[33] A. Erdohelyi, K. Fodor, G. Suru, Appl. Catal. A: Gen. 139 (1996) 131–147.
[34] M. Haneda, T. Fujitani, H. Hamada, J. Mol. Catal. A: Chem. 256 (2006) 143–148.
[35] F.J.C.M. Toolenaar, A.G.T.M. Bastein, V. Ponec, J. Catal. 82 (1983) 35–44.
[36] K. Tanaka, K.L. Watters, R.F. Howe, J. Catal. 75 (1982) 23–38.
[37] K.J. Lyons, J. Xie, W.J. Mitchell, W.H. Weinberg, Surf. Sci. 325 (1995) 85–92.
[38] M. Sushchikh, J. Lauterbach, W.H. Weinberg, Surf. Sci. 393 (1997) 135–140.
[39] A. Zecua-Fernández, A. Gómez-Cortés, A.E. Cordero-Borboa, A. Vázquez-Zavala, Appl. Surf. Sci. 182 (2001) 1–11.
[40] S.A. D'Ippolito, V.M. Benitez, P. Reyes, M.C. Rangel, C.L. Pieck, Catal. Today 172 (2011) 177–182.
[41] M. Boudart, A. Aldag, J.E. Benson, V.A. Dougharty, C.G. Harkings, J. Catal. 6 (1966) 92–99.
[42] M. Boudart, Proceedings of the 6th International Congress of Catalysis, The Chemical Society, London, 1976, pp. 1–9.
[43] W.M.H. Sachtler, R.A. van Santen, Adv. Catal. 26 (1977) 69–119.
[44] R. Coekelbergs, A. Frennet, G. Lienard, P. Resibois, J. Phys. Chem. 39 (1963) 585–591.
[45] J.A. Dalmon, G.A. Martin, J. Catal. 66 (1980) 214–221.
[46] F.G. Gault, Adv. Catal. 30 (1981) 1–95.
[47] X. Zhu, M. Shen, L.L. Lobban, R.G. Mallinson, J. Catal. 278 (2011) 123–132.
[48] T. Montanari, R. Matarrese, N. Artioli, G. Busca, Appl. Catal. B 105 (2011) 15–23.
[49] J.G. van Senden, E.H. van Broekhoven, C.T.J. Wreesman, V. Ponec, J. Catal. 87 (1984) 468–477.
[50] E. Fulop, V. Gnutzmann, Z. Paal, V. Vogel, Appl. Catal. 66 (1990) 319–336.
[51] P.T. Do, W.E. Alvarez, D.E. Resasco, J. Catal. 238 (2006) 477–488.
[52] J.H. Sinfelt, Adv. Catal. 23 (1973) 91–127.
[53] M.J. Dees, V. Ponec, J. Catal. 115 (1989) 347–355.
[54] G. Maire, G. Plouidy, J.C. Prudhomme, F.G. Gault, J. Catal. 4 (1965) 556–569.
[55] M.J. Dees, M.H.B. Bol, V. Ponec, Appl. Catal. 64 (1990) 279–295.
[56] M. Santikunaporn, J.E. Herrera, S. Jongpatiwut, D.E. Resasco, W.E. Alvarez, E.L. Sughrue, J. Catal. 228 (2004) 100–113.
[57] E.F. Sousa-Aguiar, C.J.A. Mota, M.L. Valle Murta, M. Pinhel da Silva, D. Forte da Silva, J. Mol. Catal. A: Chem. 104 (1996) 267–271.
[58] R.C. Schucker, J. Chem. Eng. Data 26 (1981) 239–241.
[59] S.A. D'Ippolito, L.B. Gutierrez, C.L. Pieck, Appl. Catal. A: Gen. 445–446 (2012) 195–203.
[60] J.M. Parera, N.S. Fígoli, in: G.J. Antos, A.M. Aitani, J.M. Parera (Eds.), Catalytic Naphtha Reforming: Science and Technology, Marcel Dekker Inc., New York, 1995 (Chapter 3).